Iraqi National Journal of Earth Science, Vol. 26, No. 03, 2026 (112-127)

Iraqi National Journal of Earth Science

www.earth.uomosul.edu.iq

Speleological Insights into Bestoon Cave: A Case Study from the Bradost Mountain, Northeastern Iraq

Mahdi Mohammed Pirot [1*], **Kamal Kolo** [2]

mahdi.pirot@soran.edu.iq kamal.kolo@soran.edu.iq

[1] *Department of Petroleum Geosciences, Science Faculty, University of Soran, Erbil, Iraq.*
[2] *Scientific Research Centre, Soran University, Erbil, Iraqi-Kurdistan Region, Iraq.*

Received: 17 April 2025 Received in revised form: 19 June 2025 Accepted: 10 August 2025
Available online: 01 July 2025

Abstract

The Bestoon Cave represents a geologically and archaeologically important karstic system formed within the Upper Cretaceous Bekhme Formation through long-term carbonate dissolution and secondary mineral deposition. The cave is located near the top of Mount Bradost in the Iraqi Kurdistan Region at an altitude of 1506 meters above sea level. This research investigates the cave's speleogenetic processes, microfabric features, and paleoclimatic significance through analyses of speleothems including flowstones, stalactites, and stalagmites. Microfabric analysis using a LEICA DM4500P polarizing light microscope for (BST-1 and BST-2) reveals distinct mineral assemblages such as dense columnar calcite, microcrystalline CaCO3, and dendrite crystal fabrics indicating fluctuating hydrological and climatic conditions. The presence of various speleothem morphologies including soda flakes, drapery, shields, cave boxwork, cave popcorn, rimstone dam, and cave pearl provides insights into the conditions of mineral deposition and water chemistry during their formation. In terms of geochemical analysis, sample BST-1 consists of 90% aragonite and 10% calcite, where the presence of calcite indicates that the original aragonitic speleothem material underwent partial recrystallization or diagenetic transport. High aragonite indicates deposition under stable conditions such as rapid precipitation from supersaturated fluids and temperature fluctuations. The sample BST-2 is composed of 100% calcite, suggesting that the mineral was formed under stable conditions favoring calcite precipitation.

Keywords:

Bestoon, Speleothem, Cave, Microfabrics, Bradost.

DOI: 10.33899/injes.v26i3.60959, ©Authors, 2026, College of Science, University of Mosul.

1. Introduction

Bestoon Cave, situated near the top of Mount Bradost in Erbil Province, Iraq (36°42'30"N, 44°23'32"E), represents one of the oldest known karstic systems in the Kurdistan Region. It is positioned at an elevation of 1,506 meters above sea level within a limestone-dominated mountain range. The cave is accessible via two primary routes: the Soran-Hawdian road, approximately 129 km north of Erbil, and the Spilk-Khalan Road, located 109 km away. The cave entrance is relatively constrained, with a height ranging from 1.3 to 2.1 meters and a width of approximately 7 meters. However, the interior expands considerably, with ceiling heights varying between 7 and 10 meters, eventually leading to a large chamber measuring between 40 and 70 meters in diameter. Despite its structural complexity, the total length of the cave remains unmeasured due to the safety measures and technical challenges encountered during fieldwork, the complex structure of the cave including narrow passages, steep inclines, and unstable areas with loose sediments or fragile speleothems, and the presence of water. (Fig.1). The cave's intricate geological framework, primarily influenced by extensive karstification processes and secondary mineral deposition, establishes it as a significant site for multi-disciplinary research in geology and archaeology (Al-Obeidi et al., 2021).

The formation of the cave is influenced by both external and internal environmental factors. Externally, regional paleoclimate patterns, precipitation, surface water movement, and tectonic activity play a significant role. Internally, factors such as rock composition, geological structure, and groundwater flow contribute to its development. The bedrock is characterized by steeply inclined, sometimes nearly vertical joints, which facilitate water movement along these fractures, accelerating rock dissolution despite the relatively rapid flow of water. The role of tectonic activity and groundwater flow in speleogenesis is well-documented in karst environments (Forti, 2005), providing a relevant framework for understanding the controlling mechanisms of Bestoon Cave's formation.

Horizontal fractures and parallel-bedding surfaces slow the movement of groundwater, allowing it to stay within the rock longer and furthering the dissolution process (Banks and Jones, 2014). The cave’s formation is also influenced by the solubility of the limestone that makes up the bedrock. Limestone dissolves more slowly than gypsum, which helps prevent cave collapse and strengthens its structure (Mohammadian et al., 2021). The solubility of limestone is much higher than that of dolomite, playing a significant role in the cave's formation, especially considering the geological makeup of the Bekhme Formation, where the upper section consists mostly of dolomite and the lower part of limestone (Liu et al., 2005; Al-Jawadi, 2023 b). This dissolution process, combined with surface water runoff, has led to the formation of Bestoon Cave in a karstic environment (Al-Obeidi et al., 2021).

This study aims to conduct a comprehensive geological analysis of Bestoon Cave with a particular focus on speleothem diversity, microfabric characteristics, geochemistry, and their implications for paleoclimate reconstruction. Specifically, it seeks to classify the various speleothem formations present within the cave, investigate the microfabric growth patterns of speleothems, and assess seasonal variations in precipitation through the analysis of fibrous calcite crystal growth (Frisia and Borsato, 2010; Fairchild and Baker, 2012). Furthermore, the study explores the cave's scientific significance in paleoclimatic studies and evaluates its potential for sustainable geo-tourism development. By examining the cave’s geological features, this research aims to elucidate the unique environmental and climatic conditions that have influenced its formation while also considering its broader applicability in speleological and paleoenvironmental studies.

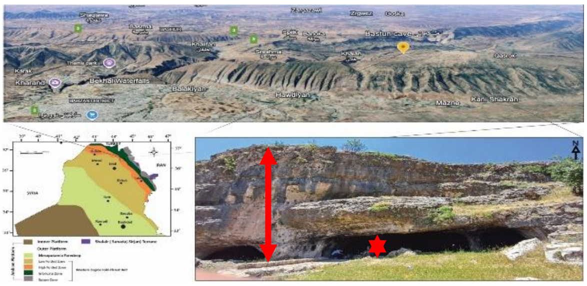

Fig. 1: Location of the study area (Bestoon Cave-Bradost Mountain): (A) tectonic zones map of Iraq (adapted from Fouad, 2015), (B) Satellite image of Bradost Mountain highlighting the cave’s location, and (C) Bestoon Cave entrance.

2. Geological Setting

Bestoon Cave is situated within the Bradost anticline, part of the Zagros Fold-Thrust Belt in northern Iraq, on the northeastern edge of the Arabian Plate within the High Folded Zone parallel to the Zagros Orogenic Belt (Jassim and Buday, 2006; Fouad, 2015; Lawa et al., 2013). The Bradost anticline is an asymmetrical double-plunging anticline characterized by an SW-verging orientation, a gentle back limb, and a nearly vertical forelimb with a tight interlimb angle. The High Zagros Fault is a nucleated array of reverse faults and back thrusts that cut through the anticline from the Triassic detachment level (Zebari et al., 2021). The syncline between the Chinara and Bradost anticlines varies in width along its length due to morphotectonic complexity, being narrower at the flanks and wider at the center between the southwestern limb of the Bradost anticline and the northeastern limb of the Chinara anticline (Shihab and Al-Obaidi, 2016; Thannoun et al., 2021).

Bestoon Cave is embedded within the bedded carbonate rocks of the Upper Cretaceous Bekhme Formation, which can be easily accessed by a paved main road from the northeastern to the southwestern limb of the anticline, near the crustal area (Stevanovic et al., 2004) (Fig. 2). The Bekhme Formation is composed of well-bedded, hard to very hard, light gray to brown limestone with very rare occurrences of dolomitic limestone (Al-Jawadi et al., 2023 b). The cave’s ceiling height varies from 7–10 meters, with visible steeply inclined to subvertical fractures, predominantly aligned with the regional strike of the Zagros Fold-Thrust Belt (Banks and Jones, 2014). The average concentration of $CaCO_3$ in the exposed limestone beds is 94.042% (Hamwandy et al., 2022), highlighting the predominance of limestone in the geological composition of Bestoon Cave (Fig. 2).

3. Materials and Methods

A detailed study is carried out on Bestoon Cave using photography and detailed measurements to document its physical dimensions and location. A global positioning system (GPS) is used to determine the exact coordinates of the cave. High-resolution images are taken from various interior angles, including different types of speleothems, entrances, and key features, ensuring a comprehensive visual record. Several speleothem samples are collected, including two stalagmites labeled BST-1 and BST-2 and one stalactite labeled BST-3, to analyze speleothem microfabric growth using a LEICA DM4500P polarizing light microscope. Sampling was done while being careful to avoid damage to the cave environment. We also took powder samples from BST-1 and BST-2 for XRD analysis to determine the chemical composition of the samples.

These records and measurements are essential for qualitative assessment of speleothem crystal fabrics like dense columnar calcite, microcrystalline calcite, and dendritic aragonite to infer seasonal changes driven by groundwater flow through fractures. Specifically, dense columnar calcite suggests stable drip conditions during wetter periods, while dendritic aragonite indicates higher Mg/Ca ratios during drier periods (Fairchild and Baker, 2012).

Due to logistical constraints, annual growth rates of calcite microfabrics and their quantitative relationships to rainy seasons (600–1,000 mm annually), temperature, and humidity are not determined; future studies should employ U-Th dating and stable isotope analysis ($\delta^{18}O$, $\delta^{13}C$) to quantify these relationships (Fleitmann et al., 2004). These data also supported spatial analysis of cave features and evaluation of Bestoon Cave's archaeological and tourism significance, highlighting its potential for paleoenvironmental research and educational outreach in the future.

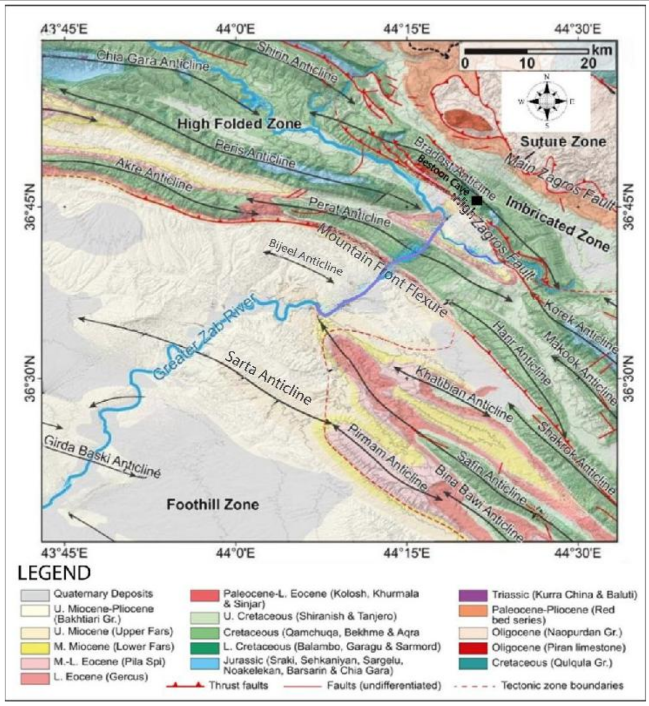

Fig. 2: Geological and location map of Bradost Anticline Mountain and Bestoon Cave (modified after Zebari et al., 2019; Zebari and Burberry, 2015; Zebari et al., 2021).

4. Climatic Conditions of Soran District

Soran district, located in northeastern Iraq within the Kurdistan Region, experiences a continental Mediterranean climate with hot and dry summers and cold and wet winters. The mountainous terrain of the region and its proximity to the Zagros Mountain Range have a significant impact on temperature fluctuations and rainfall levels (IPCC, 2021). In winter, Mediterranean storms bring moisture-rich air, causing rainfall and snowfall, while the summer monsoon is dominated by a persistent high-pressure system creating prolonged droughts (Al-Jiboori and Al-Kubaisi, 2017).

Long-term climate records and data from local weather stations indicate that Soran's mean annual temperature is approximately 13.5°C (Meteoblue, 2022). January stands as the coldest month with average minimum temperatures reaching 1.2°C, while July, the hottest month, often exceeds 40°C (Hama et al., 2014). Recorded extremes range from -15°C in winter to 44°C in summer (Tatli, 2007). Due to this extreme seasonal difference, both the spring months March and May and both the autumn months September and November offer the most comfortable weather, making them ideal for outdoor activities and tourism. Annual rainfall levels vary widely, between 600 mm and more than 1,000 mm depending largely on altitude. Maximum rainfall occurs in the Halgurd and Bradost Mountains, where orographic enhancement intensifies rainfall accumulation (Hughes, 2018). The winter months, December and February, bring the maximum amount of rainfall, often falling as snow in areas above 1500 meters elevation (Wright, 1962). In contrast, the lower foothills areas receive less moisture, averaging between 300 mm and 600 mm annually (Al-Jiboori and Al-Kubaisi, 2017). Westerly winds and Mediterranean storm systems have a significant impact on precipitation patterns, with their intensity increasing as they ascend over the region's rugged landscapes. Seasonal climate change in Soran directly affects water supply, agriculture, and biodiversity.

5. Karstification

Karst systems are known for their unique hydrology and landforms due to soluble rock and fractures that allow water to flow through. Water mainly moves vertically, with seepage, conduits, and fractures driving the flow (Ford and Williams, 2007; Perrin et al., 2003; Fairchild et al., 2006b). The time it takes for water to travel from the surface to a drip in a cave can range from hours to years depending on local conditions (Smart and Friederich, 1987). While water from different times can mix, this doesn't significantly affect shallow caves (Fairchild et al., 2000). Human activities like deforestation can change water flow in karst systems, increasing seepage into caves by reducing evapotranspiration (Fairchild et al., 2006a). Factors such as karst development, landscape features, soil properties, and soil organisms influence the recharge of aquifers, with soil fauna creating large pores that help recharge (Fairchild et al., 2006a). The karst vadose zone, which includes the soil, epikarst and transmission zone, is where ions are moved and re-precipitated (Frisia and Borsato, 2010). The epikarst, a vital water storage zone with 10-30% porosity, acts as an aquifer providing water to caves through fissures and conduits, especially after heavy rain (Fairchild et al., 2006b; Williams, 2008). It functions as a dual-porosity system, with slower flow through matrix pores and faster flow through fractures. Below it lies the transmission zone, which has limited water storage (Williams, 2008).

The karst aquifer system involves processes like photosynthesis and soil biodegradation that influence groundwater composition. As water moves through carbonate rock, it dissolves calcium carbonate, releasing ions like Ca^{2+} and HCO_3^-, which help form caverns and feed freshwater springs. Understanding these interactions is key to understanding karst hydrology (Goldscheider and Drew, 2007), as shown in Figure (3).

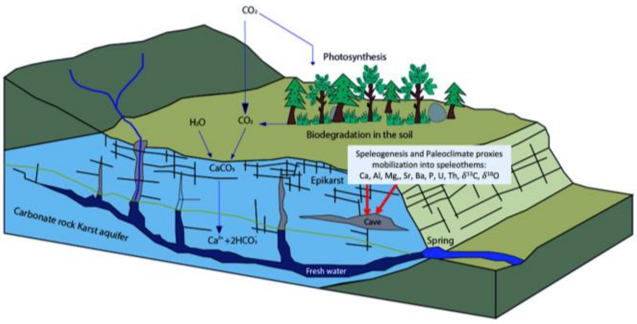

Fig. 3: A karst system's natural resources, related processes and hydrological interactions depicted schematically. Water movement and geochemical processes play a crucial part in forming the karst ecosystem, as the graphic illustrates the intricate interactions between the karst aquifer, soil, epikarst, transmission zone, and groundwater composition (Adapted after Goldscheider and Drew, 2007).

6. Formation of Speleothems

Speleothems are secondary mineral formations created by chemical interactions in caves (Hill and Forti, 1997). In karstic limestone or dolomite caves, calcium carbonate $CaCO_3$ is the primary mineral deposited. Research often focuses on three types of speleothems: stalagmites, stalactites, and flowstones (Fairchild et al., 2006a). These formations develop through complex chemical reactions involving rainwater, soil CO_2, and the surrounding rock. Rainwater, which absorbs CO_2 from the atmosphere, becomes slightly acidic, forming carbonic acid H_2CO_3 (Hendy, 1971; Dreybrodt, 1999). This acidic water dissolves minerals like calcite, $CaCO_3$, carrying calcium and other elements such as uranium into the cave (Richards and Dorale, 2003). As this water enters the cave, the CO_2 pressure drops, leading to the precipitation of calcium carbonate, then forming speleothems (Dreybrodt, 1999; Frisia and Borsato, 2010).

Rainwater interacts with increased CO_2 levels in the soil, enhancing its ability to dissolve carbonate minerals. As the water enters the cave, the CO_2 is released and calcite precipitates. This process is influenced by seasonal variations in rainfall and temperature, affecting the speleothem's growth patterns (Borsato et al., 2007; Fairchild et al., 2001; Frisia et al., 2000). The precipitation of speleothems occurs when water entering the cave is saturated with $CaCO_3$, a process influenced by the solubility of carbonates and the mildly acidic nature of meteoric water formed by CO_2 in the soil (Fairchild and Baker, 2012). As water drips into the cave, CO_2 is expelled, leading to calcium carbonate deposition on the surfaces (Lauritzen and Lundberg, 1999; Fairchild et al., 2006a). The process of speleothem formation continues as the water reaches equilibrium and begins to deposit calcium carbonate. This is a gradual process, and if the water doesn't reach equilibrium, calcite deposition won't begin until it has traveled far enough to reach that point (Dreybrodt, 2011). Crystals form when the water becomes supersaturated with calcium carbonate, a condition necessary for nucleation and crystal growth (Frisia and Borsato, 2010). Speleothems can grow as syntaxial overgrowths with crystal sizes ranging from micrometers to centimeters. Larger crystals often contain smaller ones that can only be seen under electron microscopy (Frisia and Borsato, 2010). The surface density of these crystals varies, and fluid inclusions may be trapped between them, contributing to the speleothem's growth over time (Fairchild et al., 2006a).

The formation of speleothems in Bestoon Cave, located in the Bradost Mountains of Soran District, Iraqi Kurdistan, follows the same principles. The cave, situated in karst limestone with minor dolomitic limestone, is influenced by the geological and hydrological conditions of the region. Water seeps through cracks and joints in the limestone, dissolving minerals, a critical step in speleothem formation. Temperature and rainfall changes throughout the year also affect the chemical composition of the water entering the cave. The three main stages of speleothem production dissolution, transport, and precipitation are explained through the chemical processes shown in Fig. (4).

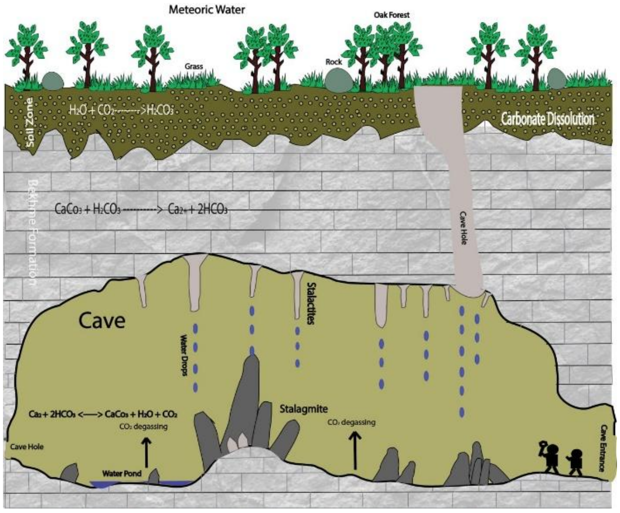

Fig. 4: Equations based on Fairchild et al. (2006a) on Bestoon Cave illustrating the relationship between meteoric water and groundwater in the soil zone, karstic zone and cave. The breakdown of organic materials in the soil zone produces CO_2, which slightly acidifies runoff waters. When limestone or dolomite rocks above a cave system in the karstic zone come into contact with this somewhat acidic water, the dissolved $CaCO_3$ in the water melts and is absorbed. The gasification of the falling fluids, as they reach the cave, causes speleothems to grow throughout it (Adapted from Frisia and Borsato, 2010).

7. Speleothem Classification in Bestoon Cave

The most commonly studied types of speleothems include stalactites, stalagmites, and flowstones, which are the primary forms previously described due to their prevalence and importance in paleoclimate research. However, additional speleothem varieties such as cave curtains (draperies), soda straws, popcorn, and helictites also occur in many cave systems and contribute to the mineralogical and morphological diversity of secondary carbonate deposits (Hill and Forti, 1997). These secondary forms, particularly soda straws and helictites, exhibit atypical growth orientations influenced by airflow or capillary forces, and while not typically used in paleoclimate reconstructions, they can reflect microenvironmental cave conditions. Among all speleothems, stalagmites and flowstones are especially valuable for paleoclimatic studies because of their stratified growth, capacity for long-term preservation, and suitability for isotopic and geochemical analyses (Fairchild and Baker, 2012; Lauritzen and Lundberg, 1999). Stalagmites are often preferred due to their vertical accretion and relatively simple morphology, which facilitate age-depth modeling and stable isotope measurements (McDermott et al., 2006). In contrast, stalactites are less frequently utilized in paleoclimate work, as their internal structure and variable growth axes can complicate stratigraphic interpretation (Hendy, 1971; Lauritzen and Lundberg, 1999).

A- Macrospeleothems in Bestoon Cave

The macrospeleothems in Bestoon Cave, notably massive stalagmites, stalactites, and flowstones, hold considerable geological significance. Their preserved structure signifies prolonged cave stability and offers insights into the mechanical strength of surrounding rocks, vital for regional engineering evaluations (Ford and Williams, 2007). Hydrogeologically, these structures record historical drip water behavior, infiltration rates, and vadose zone dynamics, rendering them significant for recreating long-term climate and groundwater variability (Fairchild and Baker, 2012). Macrospeleothems, from a mineralogical standpoint, document geochemical alterations in percolating fluids encompassing trace element fluctuations (Mg, Sr, Mn), which can enhance investigations of water-rock interactions and low-temperature carbonate mineralization processes (Frisia et al., 2000; Huang et al., 2001). Consequently, speleothems function not only as paleoclimate proxies but also as natural markers of structural, hydrogeological and geochemical processes in karst settings.

1. Flowstones

Flowstones are layers of limestone that form from flowing water saturated with calcium carbonate (Frisia and Borsato, 2010). These formations often stretch across large cave areas and can grow several meters thick. They form in response to water flow variations, and their growth rate can reach 100 micrometers per year (Frisia and Borsato, 2010). However, impurities can limit their use in dating methods like U-series dating (Fairchild et al., 2006a). Flowstones are particularly helpful for studying transitions between glacial and interglacial periods (Spötl et al., 2002; Drysdale et al., 2007), with their growth often linked to rainfall events (McDermott et al., 2006). Flowstones in several places have given Bestoon Cave a beautiful geological landscape (Fig. 5A), which has provided important insights into the cave's speleogenetic processes and mineral deposition over long periods. In areas where water has flowed down an inclined wall, it has caused the fusion of both flowstones and draperies on the walls and roof of the cave (Fig. 5B).

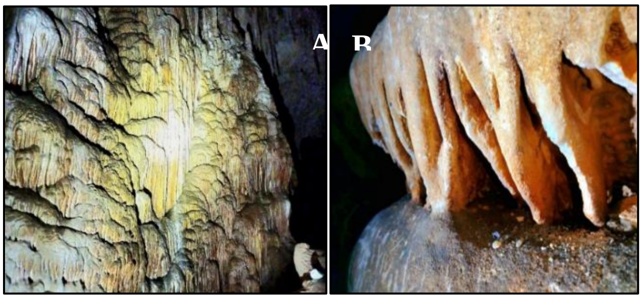

Fig. 5: Flowstones. (A) Flowstones in several areas of Bestoon Cave creating a stunning geological landscape. (B) In some locations in Bestoon Cave, flowing water has resulted in mixing of both flowstones and membranes on the walls and roof of the cave.

2. Soda Straws

According to Palmer (2007), soda straws are thin, hollow tubes that form before stalactites. Because of their fragile structure and quick growth, they are perfect for researching the early phases of speleothem development. In Bestoon Cave, soda straws are observed in several parts of the cave, which is considered an interesting discovery as these delicate structures gave beautiful and valuable insights into the geological processes of the cave. Soda straws are thin, hollow stalactite through which water slowly drips from the roof of the cave. Small calcite rings form around the edges of the drop, and over time these rings accumulate into a long columnar tube called a stalactite (Fig. 6).

Figure 6. Soda straws at Bestoon Cave: fragile, hollow stalactites formed by the slow deposition of calcium carbonate from mineral-rich dripping water from the cave ceiling.

3. Stalactites

Stalactites are conical or cylindrical formations hanging from cave ceilings. They grow by accumulating layers of calcium carbonate, and soda straw stalactites, which are hollow and fragile, develop first before becoming solid (Fairchild et al., 2006a). These formations primarily provide data on recent climate changes (Fairchild et al., 2006a) and often have annual growth bands (Huang et al., 2001; Fairchild et al., 2009). The stalactites in Bestoon cave are a beautiful geological sight. They appear in several ways, as shown in that they grew in the form of tubes down the cave (Fig. 7A), and in some places the stalactites formed in the shape of carrots (Fig. 7B). They formed when mineral-rich water flowed and dripped through the fractures in the cave. Each drop leaves some amount of calcium carbonate $CaCO_3$ and often forms in long forms or tubes like carrot shapes.

Fig. 7: Stalactites in Bestoon Cave as a beautiful geological sight. (A) Several ways of appearance as shown in those stalactites grown in the form of tubes down the cave. (B) Stalactites in some places formed in the shape of carrots.

4. Stalagmites

Stalagmites are formations that rise from cave floors, typically directly beneath stalactites. They grow in a cylindrical or conical shape and develop as calcium carbonate precipitates from water dripping above (Fairchild et al., 2006a). Stalagmites can vary in shape depending on the drip height and flow characteristics (Fairchild and Treble, 2009), and their simple form makes them useful for paleoclimate studies (Fairchild et al., 2006a). Stalagmites are found at several sites in Bestoon Cave, which is a significant geological feature and provides critical insight into the cave's speleogenetic processes and long-term mineral deposition. Two stalagmite samples, BST-1 and BST-2, are analyzed for crystal fabrics and mineral composition, offering preliminary paleoenvironmental insights, but quantitative paleoclimate reconstructions have not been performed yet. We also recommend future isotopic and dating studies to address this gap. The stalagmites grew upward and formed on the floor of the cave when mineral-rich water dripped from the ceiling or from hanging stalactites (Fig. 8).

Figure 8. Stalagmites at Bestoon Cave formed through the gradual deposition of calcium carbonate $CaCO_3$ from droplets of mineral-rich water.

5. Columns

Columns are neither stalactites nor stalagmites, but both continue to grow in opposite directions, and both may eventually merge to form a column or column of rock that becomes large and dense (Hill and Forti, 1997). The columns in Bestoon cave have given the cave a significant geological view (Fig. 9), providing valuable insights into the speleogenetic workings of the cave and mineral deposition. The columns are speleothems that form when they reach to the bottom of the cave like stalactites hanging from the ceiling (Fig. 9A). Also, in some places with stalagmites rising from the ground growing vertically and eventually united (Fig. 9B), and from the bottom of the cave to the top forming a continuous cylindrical structure 10 to 14 meters high from the ground to the bottom of the cave and 50 cm to more than 5 m in diameter. These structures were deposited as a result of gradual deposition of calcium carbonate or other minerals by water dripping from the cave ceiling over an extended period of time.

Fig. 9: Pillars of Bestoon Cave are prominent speleothems formed through the gradual deposition of calcium carbonate $CaCO_3$ from dripping water. (A) Structures grow as the stalactites extend downwards. (B) Stalagmites grow upwards, eventually coalescing to form continuous columnar structures reaching heights of 10 to 14 meters and diameters of 50 cm to more than 5 meters.

6. Draperies

Draperies that are formed of calcite develop when calcite-rich water droplets travel along a slanted cave ceiling before dripping to the floor, depositing minerals along their path. Over time, these lines create "draperies" or "cave bacon." Due to its striking resemblance to its namesake, this type of speleothem is found in nearly every cave on Earth and is widely recognized for its distinctive appearance (Palmer, 2007). In Bestoon Cave, draperies are observed at several places in the cave as a significant geological phenomenon that provides important insights into the hydrological action and mineral deposition of the cave. Cave draperies are thin, wavy membranes of calcite $CaCO_3$ or other minerals that have formed as mineral-rich water along the surface of the cave walls or roof (Fig. 10).

Fig. 10. Bestoon Cave draperies, mineral-rich water seeped along the cave's walls or roofs forming thin and wavy calcite $CaCO_3$ bacons.

7. Rimstone Dams

Calcite barriers, termed "gours" or "rimstone dams," create tiered water-filled basins in underground streams, offering significant insights into the dynamics of water flow, mineral deposition, and hydrological patterns (Ford and Williams, 2007). A notable rimstone dam is identified in Bestoon Cave, providing hydrogeological insights into the dynamics of the cave's karst aquifer (Fig. 11A). The substantial dimensions of this rimstone dam imply an extended formation duration characterized by continuous high-water flow and rich in dissolved mineral ions, signifying a vigorous karst aquifer under more humid paleoenvironmental circumstances. Conversely, smaller rimstone dams (Fig. 11B) indicate abbreviated formation durations, less water flow, and decreased mineral content, possibly linked to arid conditions or modified groundwater routes. The changes in rimstone dam morphology offer essential evidence of changing hydrological conditions inside Bestoon Cave, so enriching our comprehension of its speleogenetic and paleoenvironmental history.

Fig. 11: A unique rimstone dam at Bestoon Cave offering important insights into the processes of mineral deposition and cave *hydrology*. (A) Large rim rock dams may be indicative of stronger water flow, a longer formation period, and mineral-rich water. (B) Smaller rimstone dams may be indicative of a shorter formation period, variable flow, and less mineral-rich water.

8. Cave Pearls

Small spherical structures called cave pearls are formed in shallow ponds. Their development techniques and concentric layers shed light on the agitation and water chemistry of cave habitats (Hill and Forti, 1997). Cave pearls have been found in Bestoon Cave, which is an unusual finding because these cave pearls are rare and provide an interesting insight into the geological processes of the cave. Cave pearls are tiny rounded speleothems formed when mineral-rich water dripped onto loose grains of sand, causing layers of calcite or other minerals to roll over and build up over time. These pearls often grow in pools where the movement of water keeps them in motion, allowing them to grow into a smooth and spherical shape, as discovered in the pool of no water (Fig. 12).

Fig. 12: Cave pearls from Bestoon Cave are smooth, rounded speleothems formed in shallow pools of water where mineral-rich droplets cover small particles with layers of calcite.

9. Cave Shields

Cave shields, typically occurring in pairs, are disk-shaped calcite formations with a narrow space between them, formed when water seeps through fissures in the cave ceiling, depositing minerals in a circular pattern (Palmer, 2007). Due to logistical constraints, precise size measurements are lacking. For the future studies should quantify their dimensions to enhance understanding of their formation dynamics. Interestingly, the cave shields are observed in Bestoon Cave as rare structures, giving interesting insights into the geological processes of Bestoon Cave. The cave shield has a disc-shaped structure grown in pairs with a narrow gap between them. They were formed when oversaturated dense water seeped through fine cracks in the cave roof, and minerals such as calcite were deposited in concentric circles. The presence of cave shields at Bestoon Cave suggests that the cave had a continuous flow of water through specific passageways over an extended period (Fig. 13).

Fig. 13: Cave shields at Bestoon Cave are rare speleothems formed when mineral-rich water seeped through a crack in the cave wall and calcite deposited in thin, disc-like formations.

10. Cave Popcorn (Coralloid)

Cave Popcorn is a special kind of speleothem that is distinguished by tiny, popcorn-like, knobby, or spherical forms. Small deposits of calcite or other minerals are left behind as water evaporates or splashes on cave walls, floors, or other speleothems, where these formations usually originate (Hill and Forti, 1997). In Bestoon Cave, the popcorn is seen in several places, giving an interesting feature to the cave's unique geology. The cave popcorn at Bestoon Cave is characterized by small spiky and spherical structures had grown on the cave wall (Fig. 14).

Fig. 14: Popcorn from Bestoon Cave, which is a type of speleothem formed by mineral deposits from dripping water.

11. Cave Boxwork

Boxwork's name is derived from its resemblance to a network of post office boxes. It consists of intricate patterns of fins or plates that extend outward from bedrock surfaces, including walls, ceilings, speleothems, or floors. While boxwork can form from any mineral that is more resistant than the surrounding rock, calcite is the most commonly observed mineral. Boxwork is the result primarily of erosive forces on the bedrock. Boxwork is a good example of how minerals infill fractures and then the limestone is eroded (Hill and Forti, 1997). The Cave Boxwork found in Bestoon Cave consists of intricate patterns of plates that extend outward from bedrock surfaces formed from some mineral that is more resistant than the surrounding rock (Fig. 15).

Fig. 15: Cave Boxwork from Bestoon Cave, which is a type of Speleogen formed by intricate patterns of plates that extend outward from bedrock surfaces.

B. Microfabrics and Geochemistry of Bestoon Speleothems

1. Microfabrics of Bestoon Speleothem

For microscopic examination, we collected stalagmite samples BST-1 (Fig. 16A) and BST-2 (Fig. 16B), and stalactite sample BST-3 as shown in Figure (16C) from Bestoon Cave. Each splits vertically into two parts, and several thin sections were made for detailed microfabric analysis. In Stalagmite BST-1, the layers become progressively finer and more fragile, which is characterized by a grading of fine material indicating a slower and more gradual accumulation of minerals. In the upper part of BST-1 (Fig. 17A), the fabrics are dense columnar calcite (Cc). This section of BST-1 consists of tightly packed calcite crystals with a low length-to-width ratio (<6:1 senso Frisia); and in Figure (17A), a layer of microcrystalline $CaCO_3$ (Mc) between columnar calcite (C) above and below separates two generations of short columnar calcite fabrics. The crystal boundaries are well defined but show rugged contacts. Some crystal boundary contacts (lower-left) are separated by fine micrite material (yellow arrow). In Figure. (17B), another type of columnar calcite can be seen, classified as fascicular columnar optical calcite (Frisia, 2015), which is characterized by special forms of calcite crystals that appear twisted under the microscope. Furthermore, the crystal edges vary from straight to serrated, reflecting changes in crystallization conditions.

The color and layering variations of the stalagmite (BST-2) indicate changes in the environment over time. Light bands in the speleothem likely indicate intervals of predominantly pure calcite precipitation during wetter climatic conditions, marked by elevated and stable drip rates that promote swift carbonate deposition with minimal detrital inclusion (Fairchild and Baker, 2012; Frisia, 2015). Darker bands signify elevated levels of organic matter or detrital particles commonly linked to arid periods. Despite a reduction in overall moisture availability during these periods, speleothem deposition may nevertheless transpire due to sluggish or intermittent drip water. Reduced drip rates prolong the residence period of water on the stalagmite surface, hence augmenting the assimilation of soil-derived humic compounds and detritus into the calcite matrix (Baker et al., 1997; McDermott, 2004). Furthermore, arid conditions may facilitate surface erosion or vegetation distress, hence enhancing the mobilization of organic and clastic materials into the karst system (Spötl and Mangini, 2007; Boch et al., 2011). The existence of darker bands does not oppose less hydrological input; instead, it indicates alterations in water chemistry, drip dynamics, and catchment activities in response to arid climatic conditions. Thick layers show ongoing mineral precipitation, while thin or irregular layers show disturbances caused by drought or seasonal variations (Genty et al., 2001). The distinctive scaffold-like structure of the dendritic fabric (D) is seen in the BST-2 stalagmite (Fig. 17C). The blue arrow indicates the significant intercrystalline porosity created by the branching polycrystals that make up the fabric. Usually linked to organic matter interference, this porosity is most likely caused by microbial activity (Frisia et al., 2000). In Figure (17D), BST-2 exhibits a complex sequence of minerals including columnar calcite (C), microcrystalline $CaCO_3$ (Mc), and dendritic (D) crystals. The columnar calcite crystals are characterized by their columnar compact with no porosity between calcite crystals, and the crystals' length-to-width ratio is less than 6:1, indicating a relatively high growth rate and stable conditions (Fairchild and Baker, 2012). In contrast, the microcrystalline $CaCO_3$ layer exhibits a dense and finely crystalline texture that is visible on columnar calcite fabrics, and this suggests rapid precipitation or recrystallization (Hill and Forti, 1997). The dendritic crystals, which are detected at the lower right of the section, are branching, tree-like shapes and are indicative of rapid growth and high supersaturation, which suggests periods of rapid water flow, microbial activity, or fluctuations in water chemistry (Jones and Kahle, 1993). According to Ford and Williams (2007), the sequence of these minerals may suggest a shift in fluid chemistry or environmental conditions. The columnar calcite formed during a period of relative stability, which was followed by a rapid change or event that resulted in the formation of the microcrystalline layer, and finally, a period of high supersaturation that caused dendritic crystals to grow.

Distinct lateral development bands are observed as parallel vertical layers in the stalactite BST-3. Calcite is the main mineral deposit that is left behind after mineral-rich water evaporates, forming these bands. Light beige to golden brown color shifts are indicative of changes in impurities, environmental factors and mineral composition throughout the course of various growth phases (Tortelli and Walter, 2009). Due to the softness of the stalactite specimen BST-3, it is not possible to fabricate a thin section of the specimen. Consequently, this interpretation is based on visual inspection and available literature for the sample.

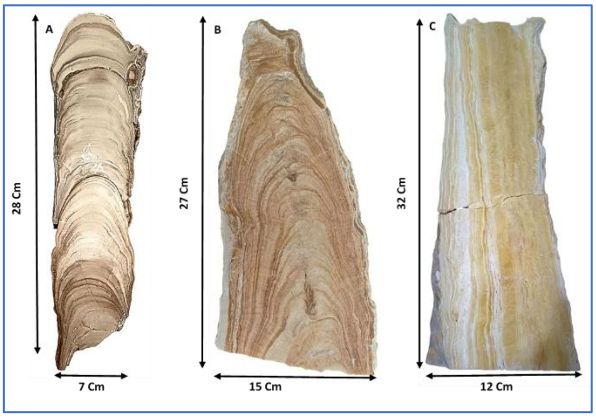

Fig. 16: Cross-section of three speleothems of the Bestoon Cave: (A) stalagmites BST-1, (B) BST-2, and (C) stalactite BST-3. The longitudinal sections reveal the speleothems' internal structures, layered pattern, and compositions, providing valuable insights into their formation processes and growth patterns.

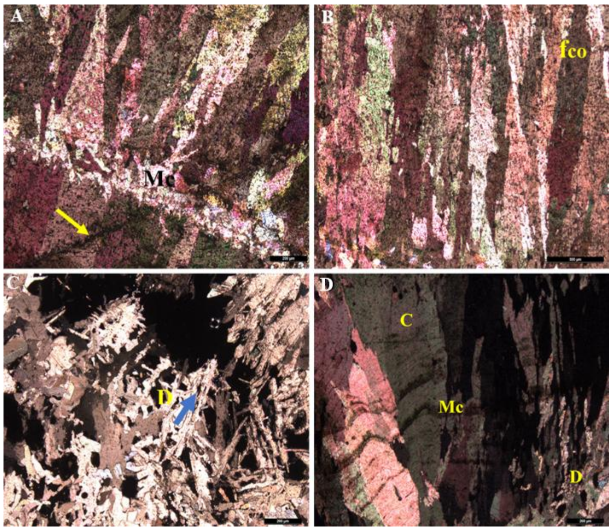

Figure 17. Microscopic examination of stalagmite samples BST-1 and BST-3 in Bestoon Cave. (A) In the upper part of BST-1, compact columnar calcite (Cc) is observed, characterized by tightly packed calcite crystals with a low length-to-width ratio (<6:1). A layer of microcrystalline $CaCo_3$ (Mc) is present between columnar calcite (C) above and below, separating two generations of short columnar calcite fabric. Crystal boundaries are well-defined but show rugged contacts, with fine micrite fabrics observed at some crystal boundary contacts (yellow arrow). (B) Columnar calcite, classified as fasicular columnar optical calcite (Frisia, 2015), which is observed in BST-1, characterized by special forms of calcite crystals that appear twisted under the microscope. (C) The crystal edges vary from straight to serrated, reflecting changes in crystallization conditions. In BST-2, a dendritic fabric (D) is observed, characterized by a scaffold-like structure with significant intercrystalline porosity, likely caused by microbial activity (blue arrow). (D) A complex sequence of minerals are observed in BST-2, including columnar calcite (C) with columnar compact and no porosity between calcite crystals, a microcrystalline $CaCO_3$ (Mc) layer with dense, finely crystalline texture, and dendritic (D) crystals with branching, tree-like shapes and high supersaturation.

2. Mineral Phase of Bestoon Speleothems

X-ray diffraction (XRD) analysis is carried out to identify the mineral composition of the Bestoon, BST-1, and BST-2 speleothem samples. The XRD results reveal a multimetallic structure consisting of calcite and aragonite. The mineralogical composition of BST-1, as determined by X-ray diffraction (XRD), is dominated by aragonite (90%) with a trace amount of calcite (10%) (Fig. 18). Aragonite is the predominant mineral in the sample, as indicated by the diffraction peaks at different 2θ angles, especially the high-intensity peaks around 26° and 45°. Calcite's presence indicates that the original aragonitic speleothem material underwent a partial recrystallization or diagenetic transition. The high aragonite content indicates deposition under circumstances that are conducive to its stability such as fast precipitation from supersaturated fluids, temperature fluctuations, or high Mg/Ca ratios. The paleoenvironmental circumstances during the creation of speleothems can be inferred from this mineralogical composition.

In BST-2, the XRD analysis reveals a (100%) dominant composition of calcite (Fig. 19). A prominent peak at 29.5° 2θ characterizes the calcite signature; it suggests that the mineral has been formed under stable conditions favoring calcite precipitation. Basically, both minerals are chemically equivalent ($CaCO_3$), but structurally different (Orthorhombic aragonite vs. trigonal calcite crystal systems). Aragonite is considered a precursor to calcite. Hence, with time, the metastable aragonite will recrystallize into stable calcite. The formation of both minerals is related to depositional conditions: temperature, drip water chemistry (acidity causing dissolution of aragonite and reprecipitation into calcite), and Mg-rich and arid cave conditions. To elaborate more, the disparity in mineral composition between BST-1 (90% aragonite, 10% calcite) and BST-2 (100% calcite) indicates divergent paleoenvironmental circumstances during deposition. The prevalence of aragonite in BST-1 may be attributed to elevated Mg/Ca ratios, enhanced evaporation, or accelerated drip rates; all are recognized to suppress calcite production and facilitate aragonite precipitation (Fairchild and Treble, 2009; Frisia et al., 2002). The pure calcite composition of BST-2 indicates more stable hydrological circumstances characterized by lower Mg/Ca ratios and a slower and equilibrium-controlled calcite precipitation (Morse and Mackenzie, 1990).

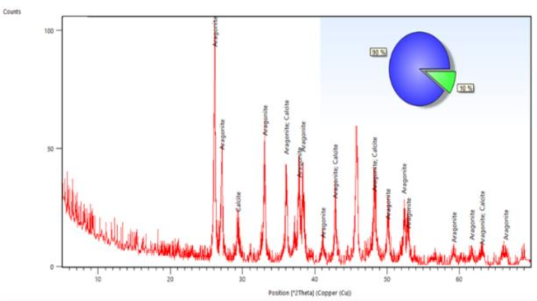

Fig. 18. XRD diffractogram of BST-1 revealing (90%) aragonite and (10%) calcite.

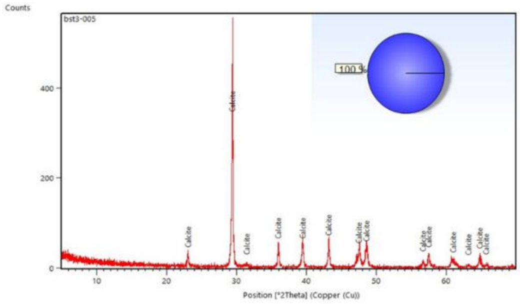

Fig. 19. XRD diffractogram of BST-2 revealing (100%) calcite.

8. Bestoon Cave Significance

Bestoon Cave, shaped by distinctive karst processes, is an important geological site that offers valuable insights into paleoclimatic variability through its stratigraphic and mineralogical features. Although no actual archaeological survey or excavations have been carried out in Bestoon Cave, the geomorphological characteristics and regional context suggest potential for future archaeological investigation, similar to the nearby Shanidar and Ashkawta Rash caves (Kerig et al., 2023). Furthermore, its impressive assemblage of stalactites, stalagmites, draperies, and other speleothems makes it a site of considerable scientific, educational, and touristic significance.

9. Conclusion

Bestoon Cave is a significant karstic cave system located in the Bradost anticline of the Zagros Fold-Thrust Belt. The dissolution of limestone and dolomite in the Upper Cretaceous Bekhme Formation formed it. Studies of the cave's speleothems, which include stalactites, stalagmites, and flowstones, have provided crucial insights into the cave's formation processes and paleoclimatic history. Mineral characteristics of Bestoon Cave are identified through microfabric analysis and XRD analysis of samples (BST-1 and BST-2), including dense columnar calcite, microcrystalline $CaCO_3$, and dendritic fabrics. These structures show how the environment has changed over time, including variations in temperature, precipitation, and microbial activity. The dark and light bands stand for dry and wet periods, respectively. These formations serve as organic paleoclimate archives. In addition, BST-1 comprises 90% aragonite and 10% calcite. Calcite indicates that the original aragonitic speleothem material underwent a partial recrystallization or diagenetic transition, and BST-2 consists of 100% calcite, suggesting that the mineral was formed under stable conditions favoring calcite precipitation. The cave's unique speleothems, such as soda straws, draperies, rimstone dams, cave popcorn, cave shields, cave boxes, and cave pearls, highlight its hydrological and geological complexity. Bestoon Cave has historical and cultural significance, and because of signs of human habitation and animal husbandry, it may have archeological potential. Its natural beauty and geological features make it the perfect place for environmentally conscious travel and educational activities. At the end, we recommend specific paleoclimate future studies using U/Th dating, stable isotopes ($\delta^{18}O$ and $\delta^{13}C$), and XRF analysis for trace elements on Bestoon stalagmites as well as drip waters.

10. Acknowledgment

We extend our sincere gratitude to the Scientific Research Center at Soran University for their invaluable assistance in utilizing the Optical Microscopy Laboratory and conducting XRD analysis.

11. References

Al-Jawadi, A.S., Al-Jumaily, I.S., Al-Dabbagh, T.H., and Davie, C., 2023 a. Evaluation of the Bekhme Dam Site – NE Iraq using the Proposed Reduction System of the Rock Mass Strength, Iraqi National Journal of Earth Science, 2023, 23(1), pp. 85–106, https://doi:10.33899/EARTH.2023.137501.1036.

Al-Jawadi, A.S., Bety, A.K., Adeeb, H.G.M., Thannoun, R.Gh., and Al-Ansari, N., 2023 b. Geological and Structural Interpretation of the Beeston Cave, Bradost Anticline, NE Iraq, Iraqi Geological Journal, 2023, 56(2F), pp. 339–349, https://doi.org/10.46717/igj.56.2F.23ms-2023-12-29.

Al-Jiboori, M.H. and Al-Kubaisi, Q.Y., 2017. Climate classification and water resources management in Iraq, Arabian Journal of Geosciences, 10(12), pp. 1-15.

Al-Obeidi, H.A., Al-Jawadi, A.S. and Al-Sanjari, A.S.A., 2021. Characteristics of Carbonate Rocks and Environmental Conditions of Some Caves, Northern Iraq, Iraqi Geological Journal, 54(2), pp. 164–175, https://doi.org/10.46717/igj.54.2E.11Ms-2021-11-27

Banks, E.W. and Jones, P.A., 2014. Hydrogeological significance of fracture systems in limestone caves, Hydrogeology Journal, 22(9), pp. 1345-1361.

Boch, R., Spötl, C. and Frisia, S., 2011. Origin and paleoenvironmental significance of lamination in stalagmites from Katerloch Cave, Austria. Sedimentology, 58(2), pp. 508–531.

Borsato, A., Frisia, S., Fairchild, I.J., Somogyi, A. and Susini, J., 2007. Trace element distribution in annual stalagmite laminae mapped by micrometer-resolution X-ray fluorescence: implications for incorporation of environmentally significant species, Geochimica et Cosmochimica Acta, 71(6), pp. 1494-1512.

Dreybrodt, W., 1999. Chemical kinetics, speleothem growth and climate change, Chemical Geology, 156(1-4), pp. 31-48.

Dreybrodt, W., 2011. Evolution of cave formations and speleothems: A modeling approach, Geochimica et Cosmochimica Acta, 75(3), pp. 765-783.

Drysdale, R.N., Zanchetta, G., Hellstrom, J.C., Fallick, A.E., McDonald, J. and Cartwright, I., 2007. Stalagmite evidence for the precise timing of North Atlantic cold events during the early last glacial, Geology, 35, pp. 77-80.

Fairchild, I.J. and Baker, A., 2012. Speleothem Science: From Process to Past Environments. Wiley-Blackwell.

Fairchild, I.J. and Treble, P.C., 2009. Trace elements in speleothems as recorders of environmental change, Quaternary Science Reviews, 28(5-6), pp. 449-468.

Fairchild, I.J., Baker, A., Borsato, A., Frisia, S., Hinton, R.W., McDermott, F. and Tooth, A.F., 2001. Annual to sub-annual resolution of multiple trace-element trends in speleothems, Journal of the Geological Society, 158, pp. 831-841.

Fairchild, I.J., Borsato, A., Tooth, A.F., Frisia, S., Hawkesworth, C.J., Huang, Y., McDermott, F. and Spiro, B., 2000. Controls on trace element (Sr–Mg) compositions of carbonate cave waters: Implications for speleothem climatic records, Chemical Geology, 166(3-4), pp. 255-269.

Fairchild, I.J., Smith, C.L., Baker, A., Fuller, L., Spotl, C., Mattey, D. and McDermott, F., 2006a. Modification and preservation of environmental signals in speleothems, Earth-Science Reviews, 75(1-4), pp. 105-153.

Fairchild, I.J., Tuckwell, G.W., Baker, A. and Worthington, S.R., 2006b. Tracing groundwater flow in karst aquifers using stable isotopes and geochemistry, Chemical Geology, 235(1-2), pp. 98-116.

Fleitmann, D., Burns, S.J. and Mudelsee, M., 2004. Holocene forcing of the Indian monsoon recorded in a stalagmite from southern Oman. Science, 300(5626), pp.1737-1739. doi:10.1126/science.1083130.

Ford, D.C. and Williams, P., 2007. Karst Hydrogeology and Geomorphology. Wiley.

Forti, P., 2005. Speleogenesis in gypsum caves: A geochemical and geomorphological approach, International Journal of Speleology, 34(1-2), pp. 15-36.

Fouad, S.F.A., 2015. Tectonic Map of Iraq, Scale 1:1,000,000, 3rd Edition, 2012. Iraqi Bulletin of Geology and Mining, 11(1), pp.1–7.

Frisia, S. and Borsato, A., 2010. Karst processes and speleothems as indicators of climate change, Geological Society, Special Publications, 336(1), pp. 171-200.

Frisia, S., 2015. Microstratigraphic Logging of Calcite Fabrics in Speleothems as Tool for Palaeoclimate Studies.

Frisia, S., Borsato, A., Fairchild, I.J. and McDermott, F., 2000. Calcite fabrics, growth mechanisms, and environments of formation in speleothems from the Italian Alps and southwestern Ireland, Journal of Sedimentary Research, 70, pp. 1183-1196.

Frisia, S., Borsato, A., Fairchild, I.J., McDermott, F. and Selmo, E.M., 2002. Aragonite–calcite relationships in speleothems (Grotte de Clamouse, France): Environment, fabrics, and carbonate geochemistry. Journal of Sedimentary Research, 72(5), pp.687–699.

Genty, D., Baker, A. and Vokal, B., 2001. Intra- and inter-annual growth rate of modern stalagmites, Chemical Geology, 176(1-4), pp. 191-212.

Goldscheider, N. and Drew, D., 2007. Methods in Karst Hydrogeology. Taylor and Francis.

Hama, S.M., Hamwandy, N.M. and Othman, N.A., 2014. Climatic variations in the Kurdistan Region, Iraq: Implications for water resources management, Journal of Hydrology, 512, pp. 417-429.

Hamwandy, N.M., Al-Jawadi, A.H. and Karim, K.H., 2022. Geochemical properties of the Bekhme Formation limestone in Iraq, Journal of Geoscience Research, 56(2), pp. 99-113.

Hendy, C.H., 1971. The isotopic geochemistry of speleothems: The interpretation of stable isotope ratios in speleothems and cave waters, Geochimica et Cosmochimica Acta, 35(8), pp. 801-824.

Hill, C.A. and Forti, P., 1997. Cave Minerals of the World (2nd Ed.). National Speleological Society.

Huang, Y., Fairchild, I.J. and McDermott, F., 2001. Seasonal variability in speleothem isotopic records: Implications for paleoclimate reconstruction, Earth and Planetary Science Letters, 194(3-4), pp. 137-148.

Hughes, R., 2018. The impact of orographic effects on precipitation in the Zagros Mountains, Journal of Climatology, 34(7), pp. 1123-1138.

IPCC (Intergovernmental Panel on Climate Change), 2021. Sixth Assessment Report: Climate Change 2021. Cambridge University Press.

Jassim, S.Z., and Buday, T. (Eds.), 2006. Geology of Iraq. Dolin, Prague and Brno, Czech Republic.

Jones, B. and Kahle, C.F., 1993. Morphology, Relationship, and Origin of Fiber and Dentrite Calcite Crystals, Journal of Sedimentary Petrology, 63, pp. 1018-1031.

Kerig, T., Lechterbeck, J., Waszk, B., Serba, P., Helms, T., Soleman, A. and Kolo, K., 2023. Geo-and ethnoarchaeological investigations of a cave in the Northern Zagros Mountains (Ashkawta Rash, Iraqi Kurdistan). Quaternary International. 10.1016/j.quaint.2023.04.012

Lauritzen, S.E. and Lundberg, J., 1999. Calibration of speleothem stable isotopes against climate records from the Holocene, Quaternary Research, 51(3), pp. 322-329.

Lawa, F.A., Koyi, H., and Ibrahim, A., 2013. Tectono-stratigraphic evolution of the NW segment of the Zagros fold-thrust belt, Kurdistan, NE Iraq. Journal of Petroleum Geology, 36(1), pp. 75–96. https://doi.org/10.1111/jpg.12543

Liu, J., Wang, Y. and Zhang, X., 2005. Dissolution kinetics of carbonate rocks in karst environments, Chemical Geology, 215(1-4), pp. 45-60.

McDermott, F., 2004. Palaeo-climate reconstruction from stable isotope variations in speleothems: a review. Quaternary Science Reviews, 23, pp. 901-918.

McDermott, F., Mattey, D.P. and Hawkesworth, C., 2006. Speleothems as high-resolution paleoclimate archives, Journal of Quaternary Science, 21(7), pp. 605-618.

Meteoblue AG., 2022. Climate data for Soran District. Available at: https://www.meteoblue.com

Mohammadian, R., Karimi, H. and Rahmati, M., 2021. Limestone dissolution and karstic cave formation: A case study from the Zagros region, Journal of Earth Sciences, 46(1), pp. 67-82.

Morse, J. and Mackenzie, F., 1990. Geochemistry of sedimentary carbonates. Developments in Sedimentology, Vol. 48. Amsterdam: Elsevier.

Palmer, A.N., 2007. Cave Geology. Dayton, OH: Cave Books, 454 P.

Perrin, J., Jeannin, P.Y. and Zwahlen, F., 2003. Impacts of climate on karst hydrology: A case study in the Swiss Jura, Hydrology and Earth System Sciences, 7(3), pp. 357-366.

Richards, D.A. and Dorale, J.A., 2003. Uranium-series chronology and environmental applications of speleothems, Reviews in Mineralogy and Geochemistry, 52(1), pp. 407-460.

Shihab, A.T. and Al-Obaidi, R.A., 2016. Geometrical and structural analysis in the High Folded Zone between Harir and Bradost anticlines, Northeast Iraq using geoinformatics techniques, Journal of Babylon University/Pure and Applied Sciences, 24(2).

Smart, P.L. and Friederich, H., 1987. Water movement in the karst vadose zone, Environmental Geology, 10(3), pp. 221-228.

Spötl, C. and Mangini, A., 2007. Speleothems and paleoglaciers. Earth and Planetary Science Letters, 254 (3-4), pp. 323–331. https://doi.org/10.1016/j.epsl.2006.11.041

Spötl, C., Unterwurzacher, M., Mangini, A. and Longstaffe, F.J., 2002. Carbonate speleothems in the dry, inneralpine Vinschgau valley, northernmost Italy: witnesses of changes in climate and hydrology since the last glacial maximum, Journal of Sedimentary Research, 72(6), pp. 793–808.

Stevanovic, Z., Markovic, M., Lawa, F.A., Ali, S.S., Karim, K.H., Omer, A., Hassan, I.O., Surdashy, A.M., Sherwani, G.H. and Aqrawi, A. M., 2004. Lithostratigraphic Map of Northern Iraq, Scale 1:50,000. Geological Survey of Iraq.

Tatli, H., 2007. Synchronization between the North Sea – Caspian pattern (NCP) and surface air temperatures in NCEP, International Journal of Climatology, 27(9), pp. 1171–1187.

Thannoun, R.Gh., Al-Jawadi, A.S., and Adeeb, H.Gh. M., 2021. Three-Dimensional Terrain Modeling for Tectonic Geomorphology of Chinara Anticline, Northern Iraq. Iraqi Geological Journal, 54(1C), pp. 52–66. https://doi.org/10.46717/igj.54.1C.5Ms-2021-03-25

Tortelli, D.M. and Walter, M., 2009. Modeling and Rendering the Growth of Speleothems in Real-time, International Conference on Computer Graphics Theory and Applications, 1, pp. 27-35.

Williams, P., 2008. The role of epikarst in karst hydrology, Journal of Hydrology, 349(3-4), pp. 290-305.

Wright, E., 1962. Climatic variations in Mesopotamia and their effects on human settlement patterns, Journal of Geology, 70(2), pp. 212-229.

Zebari, M., Preusser, F., Grützner, C., Navabpour, P., and Ustaszewski, K., 2021. Late Pleistocene-Holocene slip rates in the northwestern Zagros Mountains (Kurdistan Region of Iraq) derived from luminescence dating of river terraces and structural modeling. Tectonics, 40, e2020TC006565. https://doi.org/10.1029/2020TC006565

Zebari, M., Grützner, C., Navabpour, P., and Ustaszewski, K., 2019. Relative timing of uplift along the Zagros Mountain Front Flexure (Kurdistan Region of Iraq): Constrained by geomorphic indices and landscape evolution modeling. Solid Earth, 10(3), pp. 663–682. https://doi.org/10.5194/se-10-663-2019

Zebari, M.M., and Burberry, C.M., 2015. 4-D evolution of anticlines and implications for hydrocarbon exploration within the Zagros Fold- Thrust Belt, Kurdistan Region, Iraq. GeoArabia, 20(1), pp. 161–188.

Iraqi National Journal of Earth Science, Vol. 26, No. 03, 2026 (112-127)

Iraqi National Journal of Earth Science

www.earth.uomosul.edu.iq

منظور سبيولوجي لكهف بستون: دراسة حالة من جبل برادوست، شمال شرقي العراق

مهدى محمد بيروت [1*] ، **كمال كولو** [2]

kamal.kolo@soran.edu.iq mahdi.pirot@soran.edu.iq

[1] قسم علوم جيولوجيا النفط ، جامعة سوران، أربيل، العراق.

[2] مركز البحث العلمي، جامعة سوران، اربيل، إقليم كردستان العراق، العراق.

تاريخ الاستلام: 17 نيسان 2025 تاريخ المراجعة: 19 حزيران 2025 تاريخ القبول: 10 آب 2025

تاريخ النشر الالكتروني: 01 تموز 2026

الملخص

يمثل كهف بستون نظامًا كارستيًا ذا أهمية جيولوجية وأثرية، تشكّل ضمن تكوين بخمة من العصر الطباشيري الأعلى نتيجة ذوبان الكربونات على المدى الطويل وترسيب المعادن الثانوية. يقع الكهف قرب قمة جبل برادوست تقريبًا في إقليم كردستان العراق، على ارتفاع 1506 أمتار فوق مستوى سطح البحر. تهدف هذه الدراسة إلى تحليل العمليات المسؤولة عن نشأة الكهف (Speleogenesis) والسمات الميكروية للبنية الصخرية والأهمية المناخية القديمة له من خلال دراسة الهوابط، والصواعد، والترسيبات الانسيابية. (Flowstones) كشف تحليل النسيج الصخري الدقيق لعينات من الصواعد(BST-1) و (BST-2) عن تراكيب معدنية مميزة، مثل الكالسيت العمودي الكثيف (Dense columnar calcite)، وكربونات الكالسيوم الدقيقة التبلور (Microcrystalline $CaCO_3$)، وأنسجة البلورات المتفرعة (Dendritic crystal fabrics)، مما يشير إلى تقلبات في الظروف الهيدرولوجية والمناخية. كما أن تنوّع أشكال التكوينات المعدنية داخل الكهف مثل رقائق الصودا (Soda flakes)، والستائر (Drapery)، والدروع (Shields)، والبنية الصندوقية الكهفية (Cave boxwork)، والبوبكورن الكهفي (Cave popcorn)، والسدود الحُفرية (Rimstone dams)، واللؤلؤ الكهفي (Cave pearls)، يوفّر فهماً لظروف ترسيب المعادن وكيمياء المياه أثناء تكوّنها. أما في التحليل الجيوكيميائي، فتتكون العينة BST-1 من 90٪ أراجونيت (Aragonite) و10٪ كالسيت (Calcite)، حيث يشير وجود الكالسيت إلى أن المادة الأصلية من الأراجونيت قد خضعت لإعادة تبلور جزئي أو لتحول تكوني لاحق. ويُعزى ارتفاع نسبة الأراجونيت إلى ترسيب في ظل ظروف مستقرة، مثل التبلور السريع من محاليل فائقة التشبع أو تقلبات حرارية. في المقابل، تتكون العينة BST-2 من الكالسيت بنسبة 100٪، مما يشير إلى ترسيب في بيئة مستقرة تفضل تكوّن الكالسيت.

الكلمات المفتاحية:

بيستون، سبيليوثيم، كهف، أنسجة دقيقة، بارادوست.

DOI: 10.33899/injes.v26i3.60959,